Lifetime reduction of a quantum emitter with quasiperiodic metamaterials

Yuto Moritake,[1] Kazuyuki Nakayama,[1,2,*] Toshihiro Suzuki,[1] Hiroyuki Kurosawa,[1] Toshiyuki Kodama,[3] Satoshi Tomita,[3] Hisao Yanagi,[3] and Teruya Ishihara[1]

[1]*Department of Physics, Graduate School of Science, Tohoku University, Sendai 980-8578, Japan*

[2]*Center for the Advancement of Higher Education, Tohoku University, Sendai 980-8576, Japan*

[3]*Graduate School of Materials Science, Nara Institute of Science and Technology, Ikoma 630-0192, Japan*

(Received 23 October 2013; revised manuscript received 22 July 2014; published 26 August 2014)

Enhancement of light-matter interaction of a quantum emitter with subwavelength quasiperiodic metamaterials is proposed and demonstrated. The quasiperiodic metamaterials consist of subwavelength metal-dielectric multilayers, which are arranged into a Fibonacci lattice. The influence of Fibonacci metamaterials (FM) on the dipole emission is analyzed with a semiclassical model. The local density of states near FM is evaluated and a characteristic mode in higher wave numbers is revealed; a strong enhancement of the decay rate was predicted. A lifetime measurement is carried out and a reduction of lifetime of quantum dots on the surface of FM is observed. The enhancement of light-matter interaction arises from the localized latticelike state inherent for self-similar quasiperiodic order.

DOI: 10.1103/PhysRevB.90.075146 PACS number(s): 78.20.−e, 78.70.−g, 42.50.−p, 78.67.Pt

I. INTRODUCTION

The research on controlling spontaneous emission properties of a quantum emitter is one of the fundamental subjects in quantum optics, not only for academic interests but also for industrial developments, such as light emitting devices [1,2]. In 1946 Purcell discovered that the spontaneous emission can be changed by manipulating the photonic density of states with a resonant cavity [3]. The idea of engineering the nature of light-matter interactions was expanded and explored with artificial structures like photonic crystals [4,5]; an enhancement and suppression of spontaneous emission rate [6] and vacuum Rabi splitting [7] by photonic crystals were demonstrated. The advent of metamaterials has further extended the potential of quantum engineering, and provides novel opportunities for tailoring light with artificial structures. Various interesting researches, such as perfect superradiance [8], reversed Casimir effects [9,10], and a creation of effective electromagnetic black holes [11,12] were proposed, and quantum engineering based on metamaterials has become an active area.

In recent years, one class of metamaterials called hyperbolic metamaterials (HMMs) have captured wide research interest that supports unusual optical phenomena like negative refraction [13–15], subwavelength imaging [16–18], and nanoscale waveguides [19–22]. HMM is a highly anisotropic medium that exhibits hyperbolic dispersion relations [23]. In the case of uniaxial HMM having permittivity tensors $\varepsilon_{\parallel}$ and $\varepsilon_{\perp}$ with opposite sign, i.e., $\varepsilon_{\parallel}\varepsilon_{\perp} < 0$, the isofrequency surface of the extraordinary waves is given by

$$\frac{2k_{\perp}^2}{\varepsilon_{\parallel}} + \frac{k_{\parallel}^2}{\varepsilon_{\perp}} = \left(\frac{\omega}{c}\right)^2. \tag{1}$$

Here $k_{\parallel}$ and $k_{\perp}$ are components of the wave vector parallel and perpendicular to the anisotropy axis; ω and c are the wave frequency and speed of light. Recently, an enhancement of spontaneous emission of a quantum emitter using HMM was proposed and demonstrated [24–27]. Quantum emitters in the vicinity of HMM couple to its individual electromagnetic modes and an enhancement of the Purcell effect was observed as reduction of lifetime of quantum emitters. Especially, HMMs have the potential of broadband control of the Purcell effect due to the singularity in the density of state [28]. Metamaterials (including HMM) studied in previous works consist of subwavelength structures, whose subwavelength unit cells were aligned periodically or randomly; the functions of structural order were not focused on subwavelength structures of metamaterials.

In this work, we propose and demonstrate a scheme to enhance the light-matter interactions using HMM: introducing a quasiperiodic Fibonacci lattice into subwavelength metal-dielectric multilayered metamaterials, which we call Fibonacci metamaterials (FM) hereafter. Quasiperiodic order modifies the local density of states (LDOS) of quantum emitters near FM. Moreover, the decay rate of quantum emitters is enhanced by FM, which can be experimentally observed by a standard lifetime measurement of fluorescence of quantum dots.

II. METAMATERIAL STRUCTURES AND NUMERICAL STUDY

A. Metamaterial structures

FM is a structure stratified quasiperiodically in the order of the Fibonacci lattice, which is one of the simplest sequences in quasiperiodic lattices. The nth generation of the Fibonacci lattice is generated by the recursive formula given as

$$S_n = \{S_{n-1}S_{n-2}\}, \quad S_0 = B, \quad S_1 = A. \tag{2}$$

For example, the fifth generation of the Fibonacci lattice is ABAABABA. Here A and B correspond to metal and dielectric layer, respectively.

The structures we consider are depicted in Fig. 1(a). The silver (metal) layer and the silica (dielectric) layer are arranged into a Fibonacci lattice of generation of six. For the numerical calculation, dielectric constant of silver determined by Rakic *et al.* [29] and refractive index of silica $n_{SiO_2} = 1.45$ is used. The unit thickness of metal and dielectric layer

*Corresponding author: kaznakayama@fukuoka-u.ac.jp

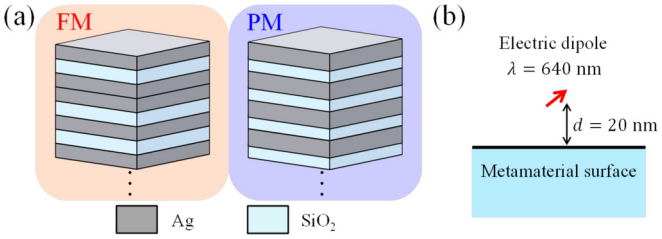

FIG. 1. (Color online) Schematics of the metamaterial structure and arrangement of the dipole. (a) Metamaterial structures composed of silver and silica layers. The layers of Fibonacci metamaterials (FM) are aligned in the order of the Fibonacci lattice and the thickness of each layer is 20 nm (left). The layers of periodic metamaterials (PM) are stratified periodically and the period is 40 nm (right). Filling factor f of PM is set to be the same as that of FM. (b) The configuration of our calculation. The dipole is placed above the material surface. The reflected field of radiation from dipole at surface affects the radiation properties of dipole.

in FM is chosen to be 20 nm. We also consider periodic metamaterials (PM) whose metal layers and dielectric layers are stratified periodically. The period of PM is 40 nm, and the number of periods is six. The total thickness of PM is slightly smaller than that of FM. Nevertheless, we can extract the essential contribution originated from the quasiperiodic structure, because the filling factor f of PM, ratio of the total thickness of metal layers against the whole thickness of metamaterials, is the same of that of FM, namely 8/13. We note that the rather low generation of the Fibonacci lattice was chosen by the sample fabrication capabilities. However, the sixth generation of FM was sufficient to verify the influence of subwavelength quasiperiodic order on light-matter interactions.

B. Numerical model

To elucidate the interaction between light and FM, we calculated the LDOS of a quantum emitter near the metamaterials by a semiclassical method developed by Chance, Prock, and Silbey [30] and Ford and Weber [31]. Figure 1(b) shows the configuration of our calculation. The dipole μ is placed in vacuum above the plane surface of metamaterials. Spacing between the dipole and the surface of metamaterials corresponds to d. The direction of dipole is parallel or perpendicular. The method takes account of the back action of the radiated field coupled with the material and provides the corrected source dipole, which well explains the radiation property near a planar surface.

The equation of motion of μ is given as

$$\frac{\partial^2\mu}{\partial t^2} + b_0\frac{\partial\mu}{\partial t} + \omega_0^2\mu = \frac{e^2}{m}E_{\mathrm{R}}. \tag{3}$$

Here b_0 and ω_0 are the decay rate and resonance frequency in vacuum. e and m are charge and mass of the electron, respectively. The term E_{R} is the reflected field which is physically equivalent to the scattering part of Green's function. The normalized total decay rate b is expressed as

$$b = 1 + \frac{e^2}{m\omega_0\mu_0 b_0}\mathrm{Im}(E_{\mathrm{R}}), \tag{4}$$

where μ_0 is amplitude of dipole. The second term in Eq. (4) represents the increased total decay rate, due to the enhancement of the medium assisted LDOS. The reflected field E_{R} is obtained by the method of Hertz vector.

Once the Fresnel coefficient for s-polarized (r_s) and p-polarized (r_p) light are given, the normalized decay rate b near a planar surface is expressed as follows:

$$b = 1 - q\,z_{\perp,\parallel}, \tag{5}$$

$$z_\perp = 1 - \int_0^\infty \frac{3}{2}\mathrm{Im}\frac{u^3}{l_1}[1 - r_p\exp(-2ilk_0d)]du, \tag{6}$$

$$z_\parallel = 1 - \int_0^\infty \frac{3}{4}\mathrm{Im}\frac{u}{l}[1 - r_s\exp(-2ilk_0d) - (1-u^2)(1 - r_p\exp(-2ilk_0d))]du, \tag{7}$$

$$l = -i\sqrt{1-u^2}. \tag{8}$$

Here q is quantum yield of emitters. The integration variable u is the component of the wave number (of the dipole field) in the plane of the surface, normalized with respect to the far-field wave number k_0 of the radiation field in vacuum; thus $u = k_x/k_0$. The integrands in Eqs. (6) and (7) correspond to the local density of states $LD(u)$, which is the measure of interaction strength of photon and material [31]. The polarization of the dipole emitter is assumed to be random; the result of ensemble measurement of decay rate b_{iso} is given by the average of perpendicular and parallel polarizations,

$$b_{\mathrm{iso}} = \tfrac{1}{3}b_\perp + \tfrac{2}{3}b_\parallel. \tag{9}$$

C. Electromagnetic states in FM

Figure 2 shows the calculated LDOS spectra for FM (red) and PM (blue) structures as a function of in-plane wave vector normalized by the free space wave number ($u = k_x/k_0$). The distance between dipole and the surface of metamaterials d was set to 20 nm. The emission wavelength λ of the dipole was 640 nm [Fig. 1(b)]. At the wavelength 640 nm, the real part of effective permittivity of metamaterials (FM and

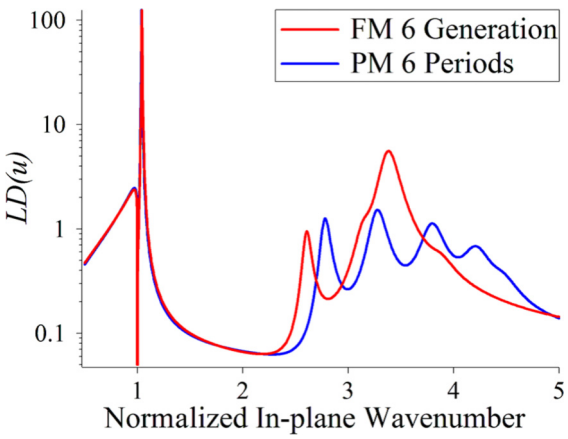

FIG. 2. (Color online) Calculation of LDOS spectra of the dipole near the metamaterials. Red line is the result for FM of sixth generation. Blue line is the result for PM of six periods. Horizontal axis corresponds to in-plane wave number u of dipole normalized by free space wave number. Significant peak is seen at $u = 3.3$ for FM.

PM) for parallel or perpendicular to the surface is $\mathrm{Re}(\varepsilon_{\parallel}) = -8.34$ and $\mathrm{Re}(\varepsilon_{\perp}) = 7.05$ [$\varepsilon_{\parallel} = f\varepsilon_{\mathrm{Ag}} + (1-f)\varepsilon_{\mathrm{SiO_2}}, \varepsilon_{\perp} = \varepsilon_{\mathrm{Ag}}\varepsilon_{\mathrm{SiO_2}}/\{(1-f)\varepsilon_{\mathrm{Ag}} + f\varepsilon_{\mathrm{SiO_2}}\}, \varepsilon_{\mathrm{Ag}} = -14.9 + 1.12i$] [23], which shows a hyperbolic dispersion relation at this wavelength.

The sharp structure around $u = 1$ in the LDOS spectra corresponds to surface plasmon polaritons excitation at a vacuum/silver interface. The electromagnetic modes with in-plane wave number larger than unity normally do not couple with free-space photons that require compensation for the momentum mismatch [32]. We can see the peaks and large value of $LD(u)$ in higher wave numbers in both PM and FM. These high-k modes correspond to the electromagnetic modes arising from the coupling of surface plasmon polaritons at each metal-dielectric interface [33]. We note that despite the difference of the detailed structure of high-k modes in PM and FM, the existence of electromagnetic modes with high wave number indicates that quasiperiodic multilayer exhibits the hyperbolic dispersion relation. Furthermore, we recognize a characteristic large peak at $u = 3.3$ in $LD(u)$ for FM.

In order to identify the specific mode with $u = 3.3$ we calculated the electric field intensity distribution of the electromagnetic mode in FM using a transfer matrix method. Figure 3(a) is a result when we ignore the losses of metals. Figure 3(b) is a result with realistic loss included. The vertical axis has a logarithmic scale. The horizontal axis corresponds to the distance from the metamaterial surface. The electric field intensity distributions in each case are very similar, and these profiles show a characteristic pattern. This mode is known as the latticelike state (LLS), which is the manifestation of self-similar property of quasiperiodic structure [34]. Numerical calculation shows that the LLS is localized around the metamaterial surface, and decays as the distance from the surface increases. Such a localized mode does not exist in PM, and exists only in FM, although not shown here.

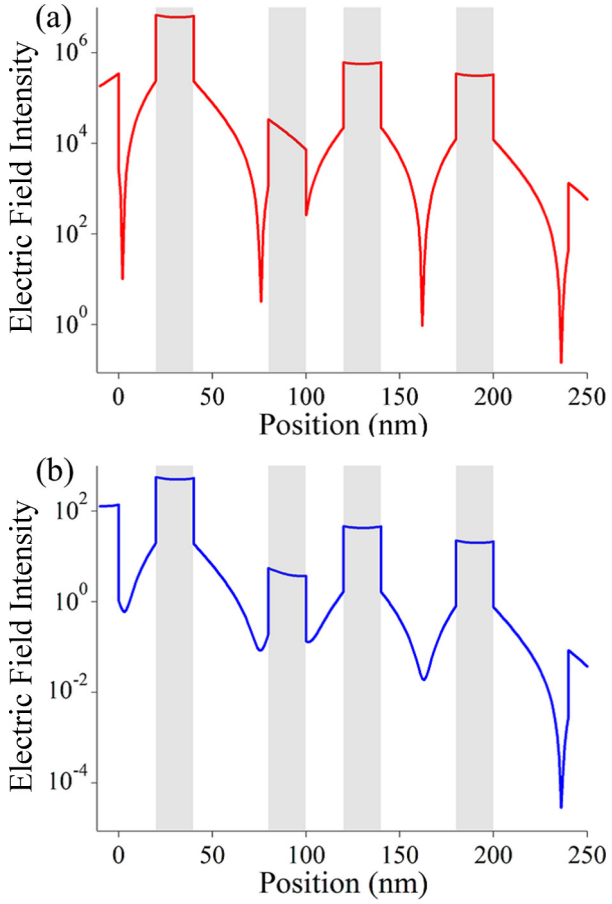

FIG. 3. (Color online) Electric field intensity distribution of LLS calculated by a transfer matrix method. The vertical axis has a logarithmic scale. The horizontal axis corresponds to the stratified direction. The shaded areas are dielectric layers. (a) Result by ignoring metallic loss. (b) Result with realistic loss [Im $(\varepsilon_{\mathrm{Ag}}) = 1.12$] included. Electromagnetic energy of LLS is localized near the surface of FM.

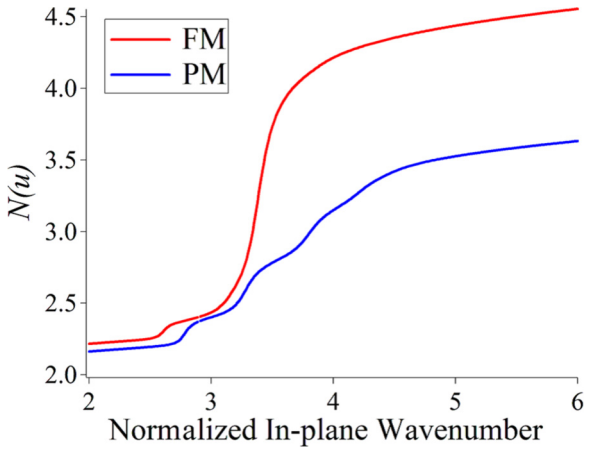

FIG. 4. (Color online) Cumulative LDOS spectra of Fig. 2 evaluated by Eq. (10). Red line is a result for FM; blue line is a result for PM. Cumulative LDOS for FM drastically increases at $u = 3.3$, which corresponds to LLS.

To evaluate the enhancement of spontaneous emission rate and the contribution of each electromagnetic mode, we define the cumulative local density of states $N(u)$ as

$$N(u) = \int_0^u LD(u')du'. \tag{10}$$

The calculated result of $N(u)$ is shown in Fig. 4. The horizontal axis corresponds to the normalized in-plane wave number u of the dipole field. Red (blue) line corresponds to $N(u)$ for FM (PM). The slope of $N(u)$ represents the contribution of the high-k electromagnetic modes in FM to total decay rate. Figure 4 shows that the total value of LDOS for FM is larger than that of PM, and this difference can be probed by quantum emitters. Moreover, the $N(u)$ for FM drastically increases at $u = 3.3$, which corresponds to LLS. Therefore, we conclude that the drastic enhancement of decay rate with FM is caused by the LLS.

III. EXPERIMENTS

A. Sample fabrication and experimental setup

The sixth generation of FM and six periods of PM were fabricated using a magnetron sputtering method [35]. A 260-nm-thick silver film was also prepared as a control sample. The structures were deposited on a silicon substrate.

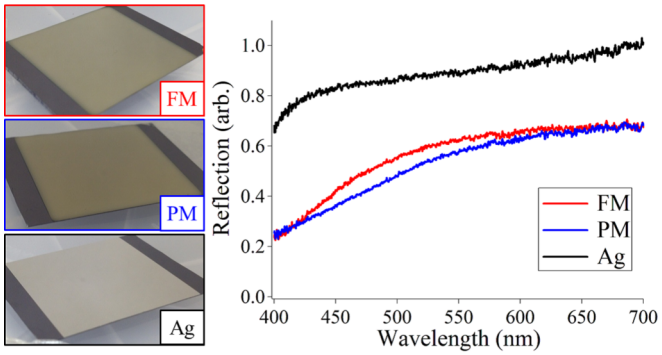

FIG. 5. (Color online) Photographs of fabricated samples (left) and reflection spectra at normal incidence (right). The effective plasma frequency of multilayer metamaterials shifts to the red side.

Finally, a 20 nm silica layer was coated on the top of each structure. The silica layer has two roles. One is to prevent surface oxidation of the top first silver layer, and the other is to suppress the fluorescence quenching effect of quantum dots by the silver surface. The left-hand side of Fig. 5 shows photographs of the fabricated samples. We cannot distinguish between FM and PM by the naked eye.

The reflection spectra of the samples for normal incidence are shown in the right-hand side of Fig. 5. From the reflection spectra, Drude tail is shifted to the red side compared with pure silver due to smaller effective free electron density in subwavelength silver/silica multilayer structures. The far-field spectroscopic property of arbitrary stratified subwavelength metal-dielectric multilayers can be characterized by an effective permittivity [36]. Therefore, the reflection spectra of FM and PM show the same far-field response irrespective of local order. This is consistent with the photographs in Fig. 5.

Colloidal core shell type CdSe/ZnS quantum dots (Sigma-Aldrich: Lumidot, emission wavelength 640 nm) were mixed with the PMMA/toluene solutions and deposited onto the samples by using a spin coating technique. A standard lifetime measurement was carried out to confirm the enhanced light-matter interaction with FM. The experimental setup is shown in Fig. 6. A blue (400 nm in wavelength) ps pulse was generated by second harmonic generation of mode-locked Ti:sapphire laser (Spectra Physics, Tsunami, 800 nm, 2 ps). The pulses were reflected by a dichroic mirror and focused

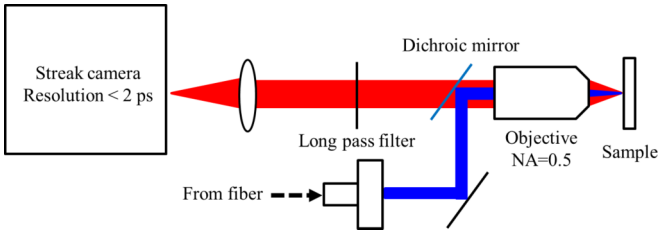

FIG. 6. (Color online) Experimental setup for a lifetime measurement of quantum dots. A blue (400 nm) pulse generated by SHG of mode-locked Ti:sapphire laser was used for excitation. Fluorescence from quantum dots was collected by an objective lens, and the time resolved lifetime measurement was carried out by a streak camera.

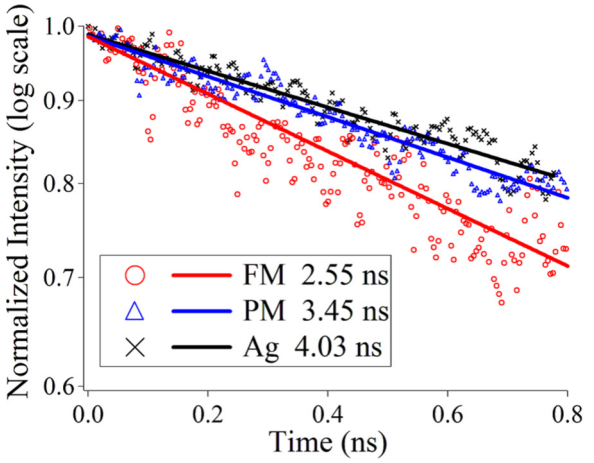

FIG. 7. (Color online) Time resolved fluorescence from quantum dots near metamaterials. Vertical axis corresponds to the normalized intensity of fluorescence in a logarithmic scale. The red circle, blue triangle, and black cross point correspond to the experimental data for FM, PM, and silver samples, respectively. Lines are the fitting results, and the estimated lifetime is indicated in the legend.

onto the sample surface to excite quantum dots, with an objective lens (Mitsutoyo: M Plan Apo NIR 100 X, NA = 0.5). The fluorescence from quantum dots was collected by the same objective lens, passed through the dichroic mirror. A time resolved measurement was performed with a streak camera (Hamamatsu photonics: C5680). Fluorescent spectra from quantum dots on each sample are almost identical. We use the data at around 640 nm for lifetime analysis.

B. Result and discussion

Figure 7 shows the result of lifetime measurement. The horizontal axis corresponds to the delay time from excitation and vertical axis corresponds to the normalized intensity of fluorescence in a logarithmic scale. The red circles, blue triangles, and black cross points correspond to the experimental data for FM, PM, and silver samples, respectively. The fluorescence decay curves showed a bimodal structure with lifetimes on the 100 ps and ns time scale. The contribution of the faster decay components (not shown in Fig. 7) was dependent on the density of quantum dots, which was minimized by reducing the concentration of quantum dots. Figure 7 displays the fluorescence data 1 ns after the excitation pulse, where the slower decay components are dominant. The fluorescence decays were described well by a single exponential function, with lifetimes indicated in the legend of Fig. 7.

First, we compare the lifetime of quantum dots near silver and PM samples. The lifetime of PM is shorter than that of silver. This result indicates that the reduction of lifetime for PM is not simply the extinction effect (quenching) due to silver, and is related to high-k modes in PM. Next we compare the lifetime of PM and FM, which shows strong reduction of lifetime compared with PM. This strong reduction insists that the integrated contribution of LDOS for FM is larger than that of PM. These experimental results are consistent with numerical ones.

TABLE I. Enhancement factor of decay rate of quantum dots near metamaterials normalized by the value for quartz substrate.

	Quartz sub.	Ag	PM	FM
Calculation	1	1.31	1.69	1.99
Experiment	1	1.80	2.11	2.85

Besides we give a comment about the intensity of fluorescence from quantum dots. The directionality of the emission from quantum emitters depends on the LDOS of the surrounding space. As a consequence quantum emitters near the surface are more likely to emit to the metamaterial side than the air side [26]. In the experiment we collect the fluorescence from the air side; therefore, large LDOS leads to reduction of the intensity. Indeed the relations between the intensity of the raw fluorescence data for each sample were FM < PM < Ag. These results also agree with the numerical predictions.

Table I shows the enhancement factor, which is the decay rate normalized by the value for quartz substrate b_{quartz}, expressed as b/b_{quartz}. The second row in the table is the numerical calculation result and the third row is the experimental result. Here, the calculated results are computed by using Eqs. (5)–(9). Quantum yield of the emitters is assumed to be 0.5, which is given in the manufacturer's catalog, although it is known that the quantum yield of an emitter is modified by the surrounding environments [27]. Therefore, for a more detailed discussion, we need to measure and analyze the apparent quantum yield, radiative, and nonradiative decay channels [27,37]. The quantum dots were assumed to be spread all over the 20-nm-thick polymer film. The uncertainty of the location was taken into account by averaging the lifetime of emitters, uniformly dispersed in the polymer layer. The normalized enhancement of the experimental results is evaluated from the inverse of lifetime. The 1.35 fold enhancement is obtained for FM compared to PM in the experiment. The overall enhancement in the experimental result is slightly large compared with the numerical evaluation. The difference can be explained by several reasons: surface roughness of the multilayered samples, overestimation of the effective distance between the emitter-doped polymer film and metamaterials, and many-body effects like fluorescence resonance energy transfer [38]. These will be the subject of future works.

Finally we discuss the qualitative physical picture of the enhancement of light-matter interaction by FM. The enhanced coupling strength can be estimated by the convolution between dipole field and electromagnetic modes in FM. Bloch-like electromagnetic modes in PM spread across the entire structure of metamaterials. Meanwhile, the LLS is localized in the vicinity of the FM surface. Therefore, the overlap between near-field components of the emissive dipole and LLS is large, and high-k modes are excited efficiently. Consequently light-matter interaction is enhanced by the LLS, which arises from the self-similar property of quasiperiodic order.

IV. CONCLUSION

In conclusion, we proposed and demonstrated an enhancement of light-matter interaction of a quantum emitter by a quasiperiodic metamaterial with the Fibonacci lattice in the subwavelength region. We analyzed the influence of FM on the dipole emission by a semiclassical model. The LDOS near FM was evaluated and a characteristic mode in higher wave numbers was revealed. The normalized total decay rate was evaluated and a significant enhancement of light-matter interaction by FM was predicted. The enhancement arises from the localized LLS inherent for self-similar quasiperiodic order. Such a localized state does not exist in periodically stratified metamaterials, and exists only in quasiperiodic metamaterials. A standard lifetime measurement with quantum dots was carried out, and a reduction of the lifetime of quantum dots in the vicinity of FM was observed.

ACKNOWLEDGMENTS

The authors would like to thank Dr. Ohno and Dr. Endo for fruitful discussions and M. Saito for his technical support. This work has been partially supported by Grant-in-Aid for Young Scientists (B), No. 24740270 from the Japan Society for the Promotion of Science (JSPS), Japan, and by the Grant-in-Aid for Scientific Research on Innovative Areas, No. 22109005 from the Ministry of Education, Culture, Sports, Science and Technology (MEXT), Japan.

[1] E. F. Schubert, *Light-Emitting Diodes*, 2nd ed. (Cambridge University Press, Cambridge, UK, 2006).
[2] C. Santori, D. Fattal, and Y. Yamamoto, *Single-photon Devices and Applications*, 1st ed. (Wiley-VCH, New York, 2010).
[3] E. M. Purcell, Phys. Rev. **69**, 37 (1946).
[4] E. Yablonovitch, Phys. Rev. Lett. **58**, 2059 (1987).
[5] S. John, Phys. Rev. Lett. **58**, 2486 (1987).
[6] P. Lodahl, A. van Driel, I. Nikolaev, A. Irman, K. Overgaag, D. Vanmaekelbergh, and W. Vos, Nature (London) **430**, 654 (2004).
[7] T. Yoshie, A. Scherer, J. Hendrickson, G. Khitrova, H. Gibbs, G. Rupper, C. Ell, O. Shchekin, and D. Deppe, Nature (London) **432**, 200 (2004).
[8] J. Kästel and M. Fleischhauer, Phys. Rev. A **71**, 011804 (2005).
[9] U. Leonhardt and T. G. Philbin, New J. Phys. **9**, 254 (2007).
[10] T.-M. Zhao and R.-X. Miao, Opt. Lett. **36**, 4467 (2011).
[11] I. I. Smolyaninov and Y.-J. Hung, J. Opt. Soc. Am. B **28**, 1591 (2011).
[12] I. I. Smolyaninov, E. Hwang, and E. Narimanov, Phys. Rev. B **85**, 235122 (2012).
[13] D. R. Smith, P. Kolinko, and D. Schurig, J. Opt. Soc. Am. B **21**, 1032 (2004).
[14] A. J. Hoffman, L. Alekseyev, S. S. Howard, K. J. Franz, D. Wasserman, V. A. Podolskiy, E. E. Narimanov, D. L. Sivco, and C. Gmachl, Nat. Mater. **6**, 946 (2007).

[15] M. Noginov, Y. Barnakov, G. Zhu, T. Tumkur, H. Li, and E. Narimanov, Appl. Phys. Lett. **94**, 151105 (2009).
[16] Z. Jacob, L. V. Alekseyev, and E. Narimanov, Opt. Express **14**, 8247 (2006).
[17] Z. Liu, H. Lee, Y. Xiong, C. Sun, and X. Zhang, Science **315**, 1686 (2007).
[18] J. Rho, Z. Ye, Y. Xiong, X. Yin, Z. Liu, H. Choi, G. Bartal, and X. Zhang, Nat. Commun. **1**, 143 (2010).
[19] V. A. Podolskiy and E. E. Narimanov, Phys. Rev. B **71**, 201101 (2005).
[20] G. Xu, T. Pan, T. Zang, and J. Sun, Opt. Commun. **281**, 2819 (2008).
[21] Y. He, S. He, J. Gao, and X. Yang, J. Opt. Soc. Am. B **29**, 2559 (2012).
[22] H. Hu, D. Ji, X. Zeng, K. Liu, and Q. Gan, Sci. Rep. **3**, 1249 (2013).
[23] A. Poddubny, I. Iorsh, P. Belov, and Y. Kivshar, Nat. Photon. **7**, 948 (2013).
[24] Z. Jacob, J.-Y. Kim, G. Naik, A. Boltasseva, E. E. Narimanov, and V. Shalaev, Appl. Phys. B: Lasers Opt. **100**, 215 (2010).
[25] M. A. Noginov, H. Li, Y. A. Barnakov, D. Dryden, G. Nataraj, G. Zhu, C. E. Bonner, M. Mayy, Z. Jacob, and E. E. Narimanov, Opt. Lett. **35**, 1863 (2010).
[26] H. N. Krishnamoorthy, Z. Jacob, E. E. Narimanov, I. Kretzschmar, and V. M. Menon, in Quantum Electronics and Laser Science Conference, 2010 (unpublished), p. JWA23.
[27] J. Kim, V. P. Drachev, Z. Jacob, G. V. Naik, A. Boltasseva, E. E. Narimanov, and V. M. Shalaev, Opt. Express **20**, 8100 (2012).
[28] Z. Jacob, I. I. Smolyaninov, and E. E. Narimanov, Appl. Phys. Lett. **100**, 181105 (2012).
[29] A. D. Rakic, A. B. Djurišic, J. M. Elazar, and M. L. Majewski, Appl. Opt. **37**, 5271 (1998).
[30] R. R. Chance, A. Prock, and R. Silbey, Adv. Chem. Phys. **37**, 1 (1978).
[31] G. W. Ford and W. H. Weber, Phys. Rep. **113**, 195 (1984).
[32] S. A. Maier, *Plasmonics: Fundamentals and Applications*, 1st ed. (Springer, New York, 2007).
[33] I. Avrutsky, I. Salakhutdinov, J. Elser, and V. Podolskiy, Phys. Rev. B **75**, 241402 (2007).
[34] M. S. Vasconcelos, E. L. Albuquerque, and A. M. Mariz, J. Phys.: Condens. Matter **10**, 5839 (1998).
[35] M. Yoshida, S. Tomita, H. Yanagi, and S. Hayashi, Phys. Rev. B **82**, 045410 (2010).
[36] D. R. Smith, D. C. Vier, T. Koschny, and C. M. Soukoulis, Phys. Rev. E **71**, 036617 (2005).
[37] V. P. Drachev, V. A. Podolskiy, and A. V. Kildishev, Opt. Express **21**, 15048 (2013).
[38] L. Novotny and B. Hecht, *Principles of Nano-Optics*, 2nd ed. (Cambridge University Press, Cambridge, UK, 2012).